

Special Issue: Brain Aging

Aging Exacerbates Obesity-induced Cerebromicrovascular Rarefaction, Neurovascular Uncoupling, and Cognitive Decline in Mice

Zsuzsanna Tucsek,^{1,*} Peter Toth,^{1,*} Stefano Tarantini,¹ Danuta Sosnowska,¹ Tripti Gautam,¹ Junie P. Warrington,^{1,2} Cory B. Giles,³ Jonathan D. Wren,³ Akos Koller,⁴ Praveen Ballabh,⁵ William E. Sonntag,¹ Zoltan Ungvari,^{1,4,6} and Anna Csiszar^{1,4,6}

¹Donald W. Reynolds Department of Geriatric Medicine, Reynolds Oklahoma Center on Aging, University of Oklahoma Health Sciences Center.

²Department of Physiology and Biophysics, University of Mississippi Medical Center, Jackson.

³Oklahoma Medical Research Foundation, Arthritis and Clinical Immunology Research Program.

⁴Department of Pathophysiology and Gerontology, Medical School and Szentágotthai Research Center, University of Pecs, Hungary.

⁵Departments of Pediatrics, Anatomy and Cell Biology, New York Medical College-Westchester Medical Center, Valhalla.

⁶Department of Physiology, University of Oklahoma Health Sciences Center.

*These authors contributed equally to this work.

Address correspondence to Zoltan Ungvari, MD, PhD, Department of Geriatric Medicine, Reynolds Oklahoma Center on Aging, University of Oklahoma HSC, 975 N. E. 10th Street-BRC 1303, Oklahoma City, OK 73104. Email: zoltan-ungvari@ouhsc.edu

Epidemiological studies show that obesity has deleterious effects on the brain and cognitive function in the elderly population. However, the specific mechanisms through which aging and obesity interact to promote cognitive decline remain unclear. To test the hypothesis that aging exacerbates obesity-induced cerebromicrovascular impairment, we compared young (7 months) and aged (24 months) high-fat diet-fed obese C57BL/6 mice. We found that aging exacerbates the obesity-induced decline in microvascular density both in the hippocampus and in the cortex. The extent of hippocampal microvascular rarefaction and the extent of impairment of hippocampal-dependent cognitive function positively correlate. Aging exacerbates obesity-induced loss of pericyte coverage on cerebral microvessels and alters hippocampal angiogenic gene expression signature, which likely contributes to microvascular rarefaction. Aging also exacerbates obesity-induced oxidative stress and induction of NADPH oxidase and impairs cerebral blood flow responses to whisker stimulation. Collectively, obesity exerts deleterious cerebrovascular effects in aged mice, promoting cerebromicrovascular rarefaction and neurovascular uncoupling. The morphological and functional impairment of the cerebral microvasculature in association with increased blood–brain barrier disruption and neuroinflammation (Tucsek Z, Toth P, Sosnowsk D, et al. Obesity in aging exacerbates blood–brain barrier disruption, neuroinflammation and oxidative stress in the mouse hippocampus: effects on expression of genes involved in beta-amyloid generation and Alzheimer’s disease. *J Gerontol Biol Med Sci*. 2013. In press, PMID: 24269929) likely contribute to obesity-induced cognitive decline in aging.

Key Words: Vascular cognitive impairment—MCI—Endothelial dysfunction—Learning and memory.

Received March 3, 2014; Accepted April 8, 2014

Decision Editor: Rafael de Cabo, PhD

CURRENTLY, close to 38% of individuals aged 65 and older in the United States are obese (1). If the current trend continues, nearly half of the elderly population will be obese by 2030 (1). Epidemiological and clinical studies, including the Framingham Offspring Study, demonstrate that a negative correlation exists between adiposity and cognitive function and that the deleterious effects of obesity on higher cortical function are exacerbated in the elderly population (2–5). It is predicted that in the obese aging baby boomer population a dramatic rise in the incidence of obesity-related cognitive impairment will occur, which

will have a significant impact on the American economy and health care system. Studies on laboratory rodents also provide evidence that deleterious cerebral effects of obesity is exacerbated in aging (6–8). Despite these advances, the underlying mechanisms by which obesity in aging impair higher cerebral function remains elusive.

The deleterious effects of obesity and obesity-related inflammation on the cardiovascular system have now been well acknowledged (9–12), and increasing evidence suggests that the vascular effects of obesity have a key role in both the development of vascular cognitive impairment (13)

and exacerbation of the symptoms of Alzheimer's disease (14–18). A significant mechanism by which obesity in aging may impair the cerebral circulation is promotion of atherosclerosis in large cerebral arteries (13). More importantly, there is growing evidence that alterations at the level of the cerebral microcirculation play a key role in neurodegeneration (17). Normal brain function is critically dependent on a continuous, tightly controlled supply of oxygen and glucose through cerebral blood flow (CBF). Although energetic demands of neurons are very high, the brain has very little reserve capacity. In humans, the cerebromicrovasculature alone consists of approximately 400 miles of capillaries, and the number of endothelial cells in the brain is very similar to that of neurons (19). Although previous studies demonstrate that a decline in capillary density in the cortex or hippocampus results in significant cognitive impairment (reviewed in Refs 20–25), there are no studies extant investigating the effects of obesity in aging on cerebral microvascular density.

In addition to age-related and obesity-induced alterations in microvascular morphology decrement of microvascular function may also contribute to impaired CBF and cognitive decline. During periods of intense neuronal activity, there is a requirement for rapid increases in oxygen and glucose delivery. This is ensured by neurovascular coupling, a vital mechanism to regulate CBF that maintains the optimal microenvironment of cerebral tissue by adjusting local blood flow to local neuronal activity (26). Because higher processes in the brain occur almost instantly, moment-to-moment adjustment of CBF via neurovascular coupling is essential for the maintenance of normal neuronal function. Although there are data available showing that feeding an high-fat diet (HFD) elicits functional impairment in cerebral microvessels (27), the synergistic effects of age and obesity on neurovascular coupling have not been elucidated.

This study was designed to test the hypothesis that aging exacerbates obesity-induced cerebrovascular rarefaction and neurovascular uncoupling. To test our hypothesis, we assessed capillary density in the cortex and hippocampus and studied expression of genes involved in regulation of angiogenesis in young and aged high-fat diet-fed obese C57BL/6 mice. To determine whether obesity in aging compromise microvascular function, we assessed neurovascular coupling by measuring changes in CBF in the somatosensory cortex elicited by whisker stimulation. Functional test for cerebromicrovascular endothelial function and oxidative stress were also performed. To substantiate the *in vivo* findings, the effects of circulating factors present in the sera on reactive oxygen species (ROS) production and angiogenic capacity of cerebromicrovascular endothelial cells (CMVECs) were assessed *in vitro*.

METHODS

Animals and Diets

In this study, we used young and aged male C57BL/6 mice (7 and 24 month old at the time of sacrifice, respectively)

from the aging colony maintained at the National Institute on Aging. Five month prior the planned sacrifice young and old animals were divided into four groups and placed on either a standard diet (SD) or HFD. The four groups were (a) young animals fed an SD (b), young animals fed an HFD, (c) old animals fed an SD diet, and 4) old animals fed an HFD, as we recently described (28). The high-fat chow, commonly used to induce obesity, delivers 60% kcal from fat, whereas the SD provides only 10% kcal from fat (D12492 and D12450B, respectively, Research Diets Inc., New Brunswick, NJ). The animals continued on the specified diets (with water and food *ad libitum*) for 5 months. Animals were housed in pairs in the Rodent Barrier Facility at University of Oklahoma Health Sciences Center on a 12-hour light–dark cycle and weighed weekly. All procedures were approved by the Institutional Animal Care and Use Committee of University of Oklahoma Health Sciences Center. Five months after starting the HFD or SD all experimental animals were fasted overnight, and serum was collected as described (8).

Behavioral Studies

At the end of the experimental period, mice were assessed for learning capacity using an elevated plus maze-based learning protocol according to the methods of Carrie and coworkers (29). In brief, a gray elevated plus maze apparatus was used. Two open arms (25 × 5 cm) and two (25 × 5 cm) closed arms were attached at right angles to a central platform (5 × 5 cm). The apparatus was 40 cm above the floor. Mice were placed individually at the end of an open arm with their back to the central platform. The time for mice to cross a line halfway along one of the closed arms was measured (transfer latency) on Days 1 and 2. Mice had to have their body and each paw on the other side of the line. If a mouse had not crossed the line after 120 seconds, the line was placed beyond it. After crossing the line, mice had 30 seconds for exploring the apparatus. Learning was defined as reduced transfer latency on Day 2 compared with Day 1. For quantitative analysis, a learning index was calculated based on relative difference in transfer latency on Days 1 and 2. A higher learning index indicates superior hippocampal function (30).

Grip Strength Test

A grip strength test was used to measure the maximal muscle strength of forelimbs of the mice. Forelimb grip strength was assessed using a grip strength meter (Chatillon Ametek Force Measurement, Brooklyn, NY). The strength measurements of each group of mice were measured 3 times by the investigator. The maximum grip strength values were used for subsequent analysis.

Measurement of CBF Responses to Whisker Stimulation and Pharmacological Studies

To assess neurovascular coupling mechanisms, at the end of the treatment period, mice in each group were

anesthetized with α -chloralose (50 mg/kg, ip) and urethane (750 mg/kg, ip), endotracheally intubated and ventilated (MousVent G500; Kent Scientific Co, Torrington, CT). Rectal temperature was maintained at 37°C using a thermostatic heating pad (Kent Scientific Co). End-tidal CO₂ (including dead space) was maintained between 3.2% and 3.7% to keep blood gas values within the physiological range (PaCO₂: ~37.5 mmHg, PaO₂: ~108 mmHg), as recently described (31). Mice were immobilized and placed on a stereotaxic frame (Leica Microsystems Inc., Buffalo Grove, IL), the scalp and periosteum were pulled aside, the skull was removed over the barrel cortex, and the dura was gently removed. The cranial window was superfused with artificial cerebrospinal fluid (composition: NaCl 119 mM, NaHCO₃ 26.2 mM, KCl 2.5 mM, NaH₂PO₄ 1 mM, MgCl₂ 1.3 mM, glucose 10 mM, CaCl₂ 2.5 mM, pH = 7.3, 37°C). The right femoral artery was cannulated for arterial blood pressure measurement (Living Systems Instrumentations, Burlington, VT). The blood pressure was within the physiological range throughout the experiment (~100–110 mmHg). A laser Doppler probe (Transonic Systems Inc., Ithaca, NY) was placed above the barrel cortex (1–1.5 mm posterior and 3–3.5 mm lateral to bregma), and to achieve the highest CBF response, the right whiskers were stimulated for 1 minute at 10 Hz from side to side. Changes in CBF were assessed above the left barrel cortex in three trials, separated by 5- to 10-minute intervals. CBF responses to whisker stimulation were repeated in the presence of the NADPH oxidase inhibitor apocynin (3 × 10⁻⁴ mol/L) administered topically to the brain surface for 30 minutes (31–33). Changes in CBF were expressed as percent (%) increase from the baseline value (34). The experimenter was blinded to the treatment of the animals.

Analysis of Microvascular Density: Immunofluorescent Labeling and Confocal Microscopy

At the end of the *in vivo* experiments, the animals were transcardially perfused with 1× heparin containing phosphate-buffered saline and decapitated. The brains were immediately removed and hemisected. From the right hemisphere, pieces of the somatosensory, the motor cortex, and the hippocampus were isolated and frozen for subsequent analysis. The left hemispheres were fixed overnight in 4% paraformaldehyde, then they were cryoprotected in a series of graded sucrose solutions (10%, 20%, and 30% overnight) and frozen in Cryo-Gel (Electron Microscopy Sciences, Hatfield, PA). Coronal sections of 70 μ m were cut through the hippocampus and stored free-floating in cryopreservative solution (25% glycerol, 25% ethylene glycol, 25% 0.2 M Na phosphate buffer, 25% distilled water) at -20°C. Selected sections were approximately 1.6 mm caudal to Bregma, representing the more rostral hippocampus. After washing (3 × 5 minutes with 1× Tris-buffered saline [TBS] + 0.25% Triton X-100 plus 3 × 5 minutes with TBS),

sections were treated with 1% of sodium borohydride solution for 5 minutes. After a second washing step (3 × 5 minutes with 1× TBS + 0.25% Triton X-100 plus 3 × 5 minutes with TBS) and blocking in 5% bovine serum albumin or TBS (with 0.5% Triton X-100, 0.3M glycine, and 1% fish gelatin for 3 hours), sections were immunostained using the following primary antibody for two nights at 4°C: mouse anti-CD31 (1:20, unconjugated; Cat N: 550274, BD Pharmingen, San Jose, CA) to label endothelial cells. The following secondary antibody was used: donkey anti-rat IgG Alexa Fluor 488 (1:1000, Cat N: A21208, Life Technologies, Grand Island, NY) or goat anti-rat IgG Alexa Fluor 568 (1:1000, Cat N: A11077, Life Technologies, Grand Island, NY). Sections were washed for 3 × 5 minutes with 1× TBS + 0.25% Triton X-100 plus 3 × 5 minutes with TBS. For nuclear counterstaining, Hoechst 33342 was used. Then, the sections were transferred to slides and coverslipped. Confocal images were captured using a Leica SP2 MP confocal laser scanning microscope.

Immunofluorescent labeling for CD31 was used to identify microvessels in the brain as we previously described (24,30). Capillary density in the CA1 region of the hippocampus, retrosplenial cortex, and corpus callosum (cc) was quantified, using stereological methods, as the length of blood vessels less than 10 μ m in diameter per volume of tissue using Neurolucida with AutoNeuron (MicroBrightField, Williston, VT). Brain regions were identified based on the study by Hof and coworkers (35). The total length of capillaries (mm) was divided by the volume of brain tissue scanned (mm³) to obtain capillary density (length per tissue volume). The density of CD31-stained capillaries was calculated within each region for each animal. The experimenter was blinded to the groups and treatments of the animals throughout the period of blood vessel staining and analysis.

Pericyte Coverage

Pericytes have key roles in maintenance of the structural integrity of the cerebral microcirculation (36). To assess age- and obesity-induced changes in pericyte coverage of microvessels, in brain sections from young and aged mice with or without HFD-induced obesity, immunolabeling for the pericyte marker platelet-derived growth factor receptor β (PDGFR β) and the endothelial marker CD31 (as described earlier) was performed. We processed tissue sections for immunolabeling using 1:50 rabbit anti-mouse PDGFR β (Cell Signaling, Danvers, MA) antibody. Sections were incubated in primary antibody for 42 hours, washed 3 × 5 minutes with 1× TBS + 0.25% Triton X-100 plus 3 × 5 minutes with TBS, and incubated for 3 hours in 1:1000 donkey anti-rabbit Alexa Fluor 555 (Cat N: A31572, Life Technologies, Grand Island, NY). For pericyte coverage, anti-PDGFR β (which is abundantly expressed in pericytes) and anti-CD31 signals from microvessels less than or equal

to 10 μm in diameter were separately subjected to threshold processing. The capillary surface area occupied by pericytes (identified as PDGFR β positive cells with a typical pericyte morphology, long processes that extend over the capillaries, and perivascular localization with a Hoechst 33342-stained prominent round nucleus) per CD31 positive capillary surface area per field was calculated. The areas occupied by the respective signals were analyzed using the area measurement tool of the MetaMorph software (version 7.7.9.0). Pericyte coverage was determined as a percentage (%) of PDGFR β positive pericyte surface area covering CD31 positive capillary surface area per field. In each animal, four randomly selected fields from the hippocampus were analyzed in six nonadjacent sections. Six animals per group were analyzed.

Quantitative Real-Time Reverse Transcription-PCR

A quantitative real-time reverse transcription-PCR technique was used to analyze mRNA expression of genes known to be involved in regulation of angiogenesis in hippocampi of mice from each experimental group as reported (8,30,37). In brief, total RNA was isolated with a Mini RNA Isolation Kit (Zymo Research, Orange, CA) and was reverse transcribed using Superscript III RT (Invitrogen) as described previously (38). Hippocampal mRNA expression of pro- and antiangiogenic genes was analyzed using validated TaqMan Gene Signature Array Micro Fluidic Cards (Angiogenesis array, Applied Biosystems) and a validated TaqMan assay for *Nox2* and a Strategen MX3000 platform, as previously reported (38). Quantification was performed using the efficiency-corrected $\Delta\Delta\text{Cq}$ method. Using the Bioconductor HTqPCR package (39), arrays were first rescaled to ΔCt values using *Ywhaz*, *B2m*, and *Hprt* as a reference, then quantile normalized. "Undetermined" Ct values were replaced with the global maximum Ct value. Differential expression significance was determined using the Bioconductor limma package, and the directionality and magnitude of the angiogenic signature were assessed using both the *t* statistic and Gene Set Enrichment Analysis (40) as implemented in the Bioconductor GSA package.

Assessment of the Effects of Circulating Factors on Endothelial Angiogenic Capacity

To investigate the influence of circulating factors present in the bloodstream of SD- and HFD-fed young and aged mice on endothelial angiogenic capacity, tube formation assay (41–43) was performed using cultured primary CMVECs treated with sera obtained from mice in each experimental group. In brief, primary rat CMVEC cultures were established as recently reported (41,44). CMVECs were initially cultured in MesoEndo Endothelial Cell Growth Medium (Cell Applications Inc.) followed by Endothelial Basal Medium supplemented with 10% fetal calf serum until the time of serum treatment, as described (45–48). For treatment, fetal

calf serum was replaced with serum (10%) collected from SD- and HFD-fed young and aged mice. Geltrex Reduced Growth Factor Basement Membrane Matrix (150 μL /well; Invitrogen, Carlsbad, CA) was distributed in ice-cold 24-well plates. The gel was allowed to solidify while incubating the plates for 30 minutes at 37°C. Then, CMVECs were seeded at a density of 5×10^4 cells/well and placed in the incubator for 24 hours. Microscopic images were captured using a Nikon Eclipse Ti microscope equipped with a $\times 10$ phase-contrast objective (Nikon Instruments Inc., Melville, NY). The extent of tube formation was quantified by measuring total tube length in five random fields per well using NIS-Elements microscope imaging software (Nikon Instruments Inc), as recently reported (43). The mean of the total tube length per total area imaged (μm tube/ mm^2) was calculated for each well. Experiments were run in quadruplicates. The experimenter was blinded to the groups throughout the period of analysis.

Assessment of the Effects of Circulating Factors on Endothelial Oxidative Stress

To investigate the influence of circulating factors present in the bloodstream of SD- and HFD-fed young and aged mice on endothelial oxidative stress, O_2^- production was assessed in cultured CMVECs treated with sera obtained from mice in each experimental group. Cellular O_2^- production was measured using the cell-permeant oxidative fluorescent indicator dye dihydroethidium (3×10^{-6} mol/L, for 30 minutes) as previously reported (28,49). Dihydroethidium fluorescence was assessed by flow cytometry as previously reported (50,51), using the Guava easy-Cyte 8HT flow-cytometer (Millipore, Hayward, CA).

Measurement of 3-Nitrotyrosine Content

To characterize the effect of obesity on cellular redox homeostasis in aging, 3-nitrotyrosine (a marker for peroxynitrite action) was assessed in homogenates of cortical samples using OxiSelect Protein Nitrotyrosine ELISA Kits (Cell Biolabs), according to the manufacturer's guidelines, as previously described (31).

Statistical Analysis

Data were analyzed by one-way ANOVA followed by Tukey post hoc tests and Pearson's correlation analysis, as appropriate. A *p* value less than 0.05 was considered statistically significant. Data are expressed as mean \pm SEM.

RESULTS

Effects of Chronic HFD and Aging on Body Mass and Neuromuscular Strength

In agreement with previous data (6,7), we found that both young and aged C57BL/6 mice fed an HFD

exhibited significant weight gain over the experimental period (Figure 1A). The relative increase in body mass (calculated as a percentage of body mass at the beginning of treatment) of HFD-fed young mice was significantly greater, compared with HFD-fed aged animals. The effects of chronic HFD feeding on the serum biochemical profile of young and aged C57BL/6 mice are shown in Supplementary Table I. We observed that obesity in aging was associated with a significant decline in grip strength, a measure of decreased neuromuscular strength (Supplementary Figure I), mimicking the phenotype described in obese elderly human participants (52).

Aging Exacerbates Obesity-induced Decline in Hippocampal Cognitive Function

To determine whether obesity in aged mice induces neurocognitive impairment, we studied hippocampally dependent learning and memory. For young control mice, transfer latency on Day 2 was significantly decreased (by ~49%), compared with Day 1 (Figure 1B), indicating an intact learning effect (learning index: 0.49). The learning indexes for young obese mice (~0.27) and aged (~0.34)

mice tended to decrease, compared with young control mice although the differences did not reach statistical significance. For obese aged mice, transfer latency was similar on Days 1 and 2 (corresponding to a learning index of ~0), indicating that these mice had significantly impaired learning ability.

Aging Exacerbates Obesity-induced Cerebromicrovascular Rarefaction and Loss of Pericyte Coverage

We determined whether obesity influences brain capillary density in aged mice. Capillaries were identified by their expression of CD31 (Figure 2A–E), using a lumen diameter of 10 μ m or less as a standard identifier. As shown in Figure 2F and G, in aged mice, obesity was associated with significant decreases in capillary length density in the CA1 region of the hippocampus and retrosplenial cortex. In contrast, obesity did not affect significantly brain capillarization in young mice. Capillary length densities in the corpus callosum were similar in each experimental group.

Because recent studies demonstrate that pericyte loss can compromise cerebromicrovascular morphology (53), we assessed age- and obesity-induced changes

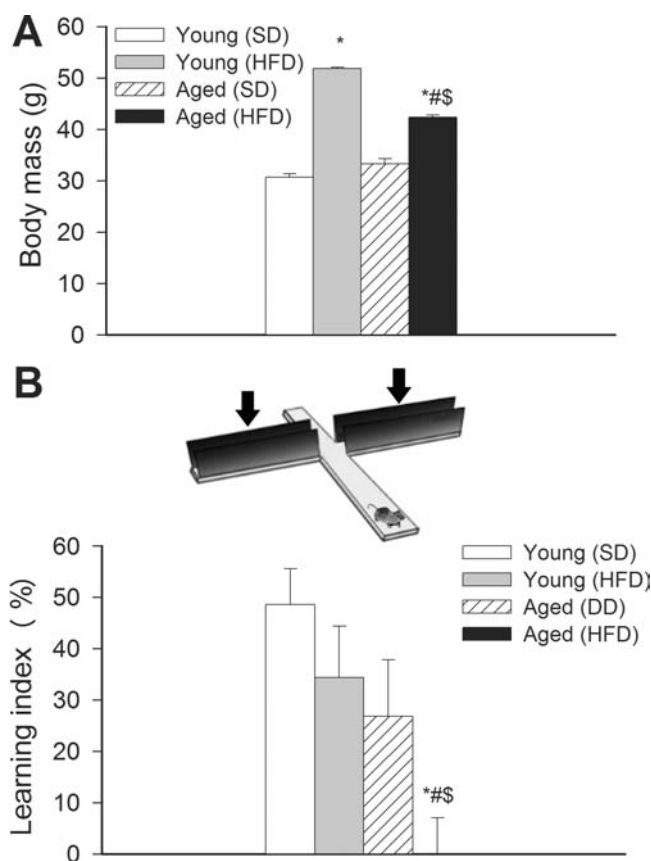


Figure 1. Obesity-related changes in hippocampal function in aging. (A) Body mass of young and aged mice fed a high-fat diet (HFD) or standard diet (SD) at the time of sacrifice. Data are means \pm SEM. * p < .05 vs young mice (SD), # p < .05 vs aged mice (SD), $\$p$ < .05 vs young mice (HFD). (B) Aging exacerbates obesity-induced cognitive impairment (elevated plus maze-based learning protocol; see Methods section for details). For obese aged mice, transfer latency was similar on Days 1 and 2 (corresponding to a learning index: ~0), indicating that these mice had significantly impaired learning ability. Data are given as mean \pm SEM. * p < .05 vs young mice (SD), # p < .05 vs aged mice (SD), $\$p$ < .05 vs young mice (HFD).

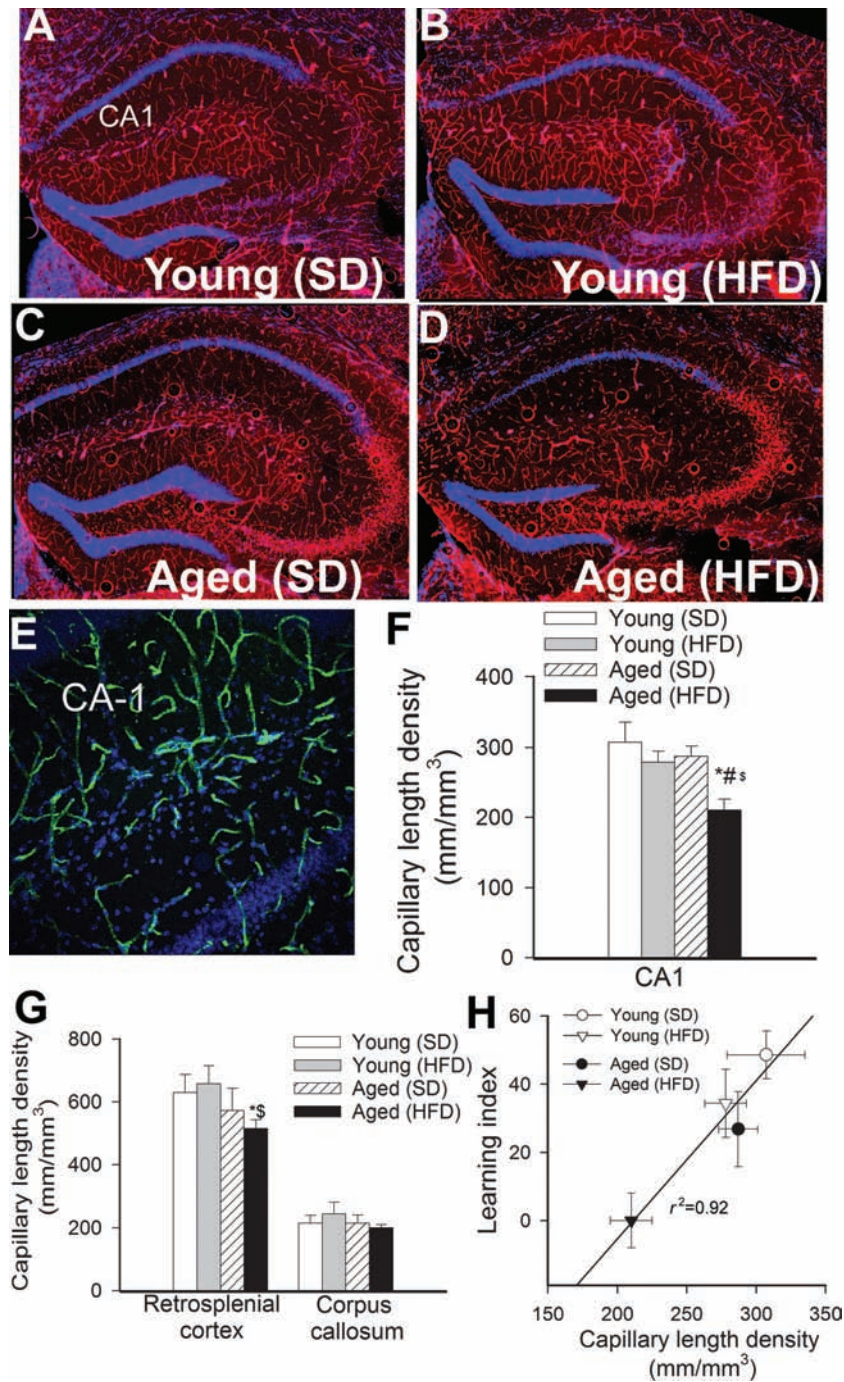


Figure 2. Obesity-induced changes in cerebral capillary density in aging. (A–D) Representative confocal images showing CD31 positive capillary endothelial cells (red) in the hippocampi of young and aged mice fed an HFD or SD. Hoechst 33342 was used for nuclear counterstaining (original magnification: $\times 5$). (E) Representative confocal microscopic analysis of CD31 positive capillaries (green) in the CA1 region of the hippocampus of an obese aged mouse (original magnification: $\times 20$). (F and G) Summary data for obesity-induced changes of capillary length density in the CA1 region of the hippocampus (F), retrosplenial cortex and corpus callosum (G) of young and aged mice. Data are given as mean \pm SEM. * $p < .05$ vs young mice (SD), # $p < .05$ vs aged mice (SD), $^{\$}p < .05$ vs young mice (HFD). (H) Relationship between capillary length density in the CA1 region of the hippocampus of young and aged mice fed an HFD or SD and the learning index obtained in these groups of animals.

in pericyte coverage of hippocampal microvessels (Figure 3). We found that obesity in young mice did not affect significantly capillary pericyte coverage. In contrast, obesity in aged mice resulted in a significant

decline in pericyte coverage of hippocampal microvessels (Figure 3). Advance age itself was associated with a slight, but significant, decline in capillary pericyte coverage.

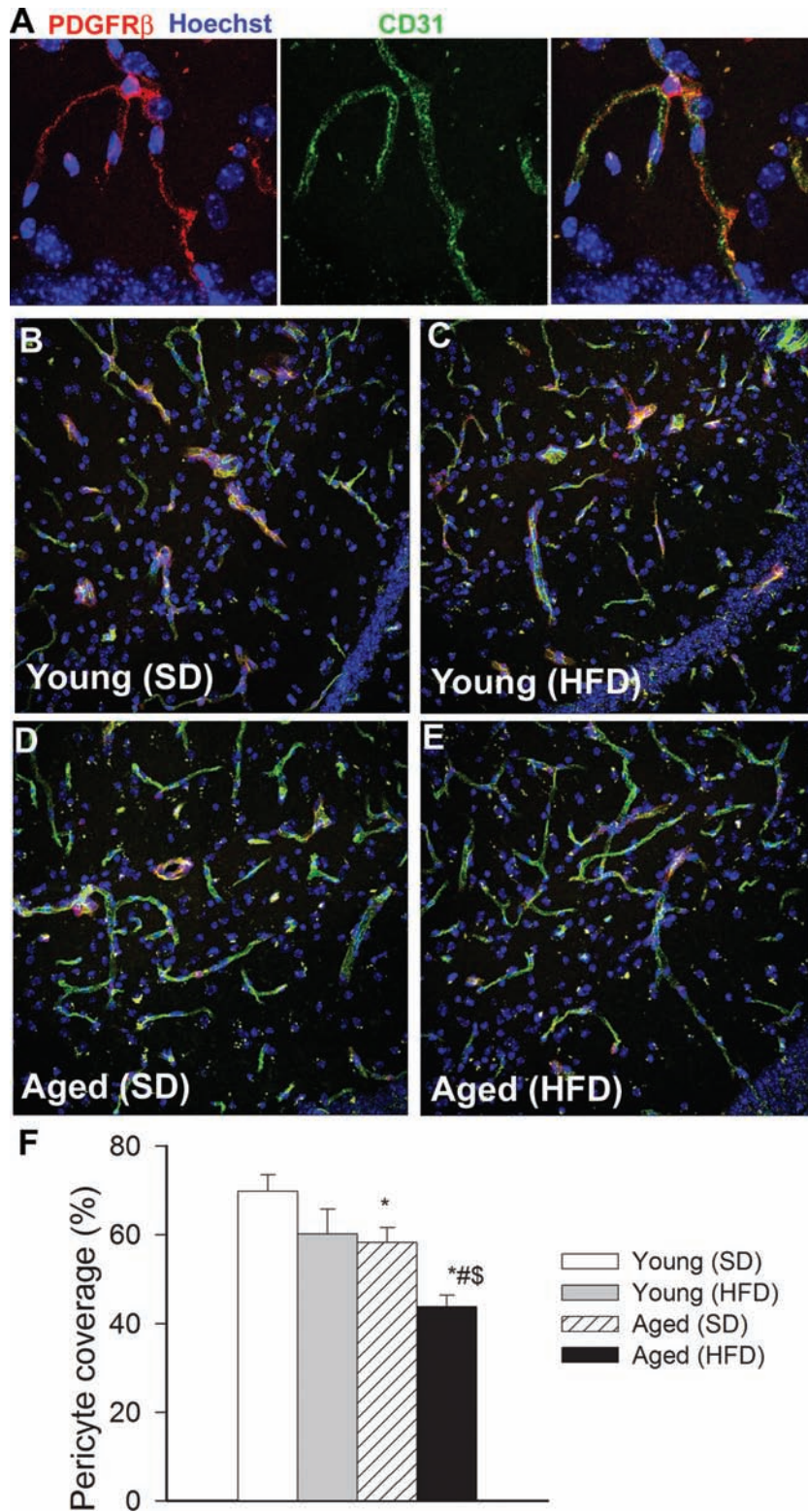


Figure 3. Obesity-induced changes in pericyte coverage of hippocampal capillaries in aging. (A) Representative confocal image showing perivascular localization of a platelet-derived growth factor receptor β (PDGFR β) expressing pericyte (red) surrounding CD31 positive capillary endothelial cells (green) in the CA1 region of the mouse hippocampus. Hoechst 33342 was used for nuclear counterstaining. (B–E) Representative confocal microscopy analysis of PDGFR β expressing pericyte coverage (red) of CD31 positive capillaries (green) in the CA1 region of the hippocampi of young SD-fed (B), young HFD-fed (C), aged SD-fed (D) and aged HFD-fed (E) animals. (F) Summary data showing obesity- and aging-dependent loss of pericyte coverage in the hippocampus (see Methods section for details). * $p < .05$ vs young mice (SD), * $p < .05$ vs aged mice (SD), * $p < .05$ vs young mice (HFD).

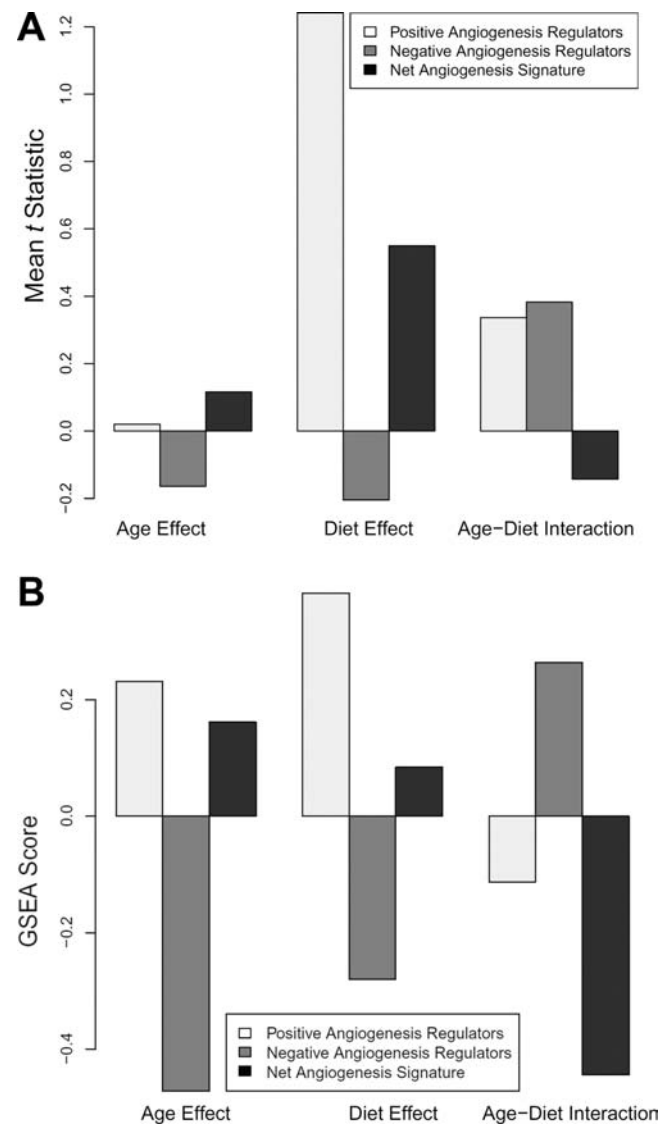


Figure 4. Panel A: Mean *t* statistic for positive and negative angiogenesis regulators and the signed aggregate of both groups. Panel B: Gene set enrichment analysis (GSEA) scores for positive and negative regulators of angiogenesis and the signed aggregate of both groups. HFD appears to increase the angiogenesis signature, age and the age–diet interaction appear to have mixed effects, whereas the age–diet interaction shows a trend toward decreased angiogenic signature. “Age Effect” refers to old vs young, “Diet Effect” refers to HFD vs control, and “Age–Diet Interaction” refers to the changes in gene expression that occur with the combination of age and HFD that cannot be accounted for by age or diet alone.

Effects of Age and HFD on Hippocampal Angiogenic Gene Expression Signature

We detected and analyzed the mRNA expression of 90 angiogenesis-associated genes in the mouse hippocampi (see online [Supplementary Data](#)). To determine whether the array data suggest a positive or negative angiogenesis signature for various conditions, genes annotated with the Gene Ontology terms for “positive regulation of angiogenesis” (GO:0045766; example: *Vegfa*) and “negative regulation of angiogenesis” (GO:0016525; example: *Thbs*) were obtained and intersected with the genes on the array. Genes annotated with both terms were removed. To assess the directionality of the angiogenesis signature, *t* statistic values were

calculated. [Figure 4A](#) depicts mean *t* statistic for positive and negative angiogenesis regulators and the signed aggregate of both groups. To interpret the gene expression data, Gene Set Enrichment Analysis scores were also calculated for positive and negative regulators of angiogenesis and the signed aggregate of both groups ([Figure 4B](#)). High-fat diet appears to increase the angiogenesis signature; age and the age–diet interaction appear to have mixed effects; however, the age–diet interaction is weakly negative, implying that age and high-fat diet do not act in a strongly synergistic manner toward altering the angiogenic gene expression signature. The effects of age and diet on individual gene expression are shown in the online [Supplementary Data](#).

Effect of Treatment With Sera From Obese Mice on Formation of Capillary-like Structures by CMVECs

When seeded onto Geltrex matrices, CMVECs treated with sera from young SD-fed mice formed elaborated capillary networks in the presence of vascular endothelial growth factor (Figure 5A). We found that treatment with sera from HFD-fed young mice did not significantly inhibit the formation of capillary-like structures by CMVECs (Figure 5B). Compared with cells treated with sera from young SD-fed mice, in CMVECs treated with sera from SD-fed aged mice, formation of capillary-like structures was significantly increased (Figure 5C). The finding, that in CMVECs treated with sera from HFD-fed aged mice formation of capillary-like structures was similar (Figure 5B), suggests that obesity-associated circulating factors do not exert antiangiogenic effects (which would explain the observed capillary rarefaction in obese aged mice).

Aging Exacerbates Obesity-induced Neurovascular Uncoupling: Role of Increased Oxidative Stress

Changes in CBF in the whisker barrel cortex in response to contralateral whisker stimulation was significantly decreased both in obese young mice and lean aged mice compared with young lean animals, indicating impaired neurovascular coupling in aging and obesity (representative tracings are shown in Figure 6A, summary data are shown in Figure 6B) (31,54). Aging exacerbated obesity-induced neurovascular uncoupling (Figure 6A and B). NADPH oxidases are important sources of ROS in the cerebral vasculature, whose increased expression and activity impairs neurovascular coupling (31,54). We found that inhibition of NADPH oxidases by apocynin significantly increased CBF responses induced by contralateral whisker stimulation in aged obese mice restoring neurovascular coupling to levels observed in young mice (Figure 6C). 3-Nitrotyrosine content in the cerebral cortex was significantly elevated in aged mice (Supplementary Figure IV), consistent

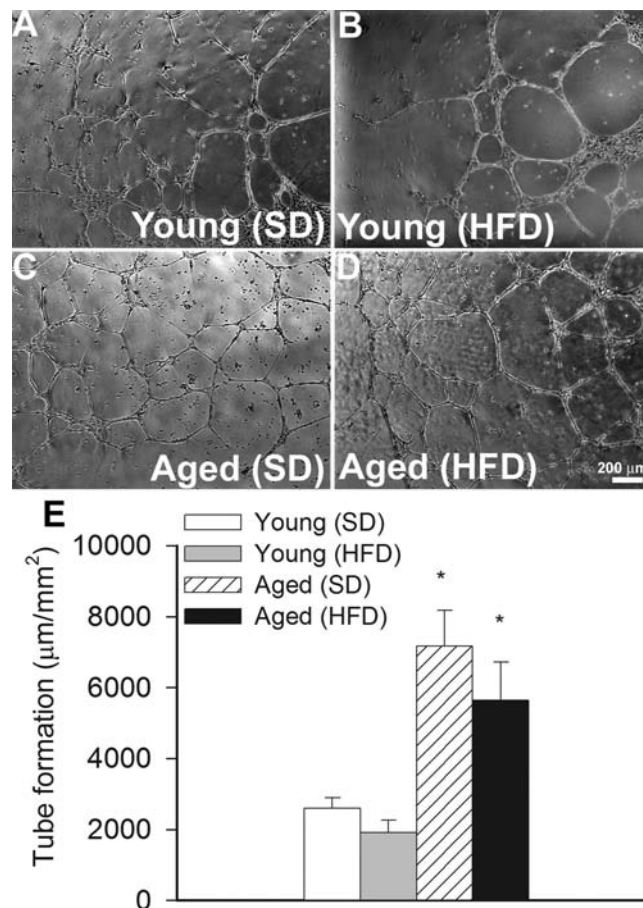


Figure 5. Effect of factors present in the circulation of young and aged obese and lean mice on endothelial angiogenic capacity. Treatment with sera collected from young mice fed an HFD does not affect formation of capillary-like structures by cerebrovascular endothelial cells (CMVECs). In contrast, treatment with sera collected from aged mice fed an SD or an HFD significantly increases endothelial angiogenic capacity. CMVECs were plated on Geltrex-coated wells, and tube formation was induced by treating cells with vascular endothelial growth factor (100 ng/mL, for 24 h). Representative examples of capillary-like structures are shown on Panels A–D. Summary data, expressed as total tube length per total area scanned (µm tube/mm²), are shown in Panel E. Data are given as means ± SEM ($n = 5$ in each group). * $p < .05$ vs control.

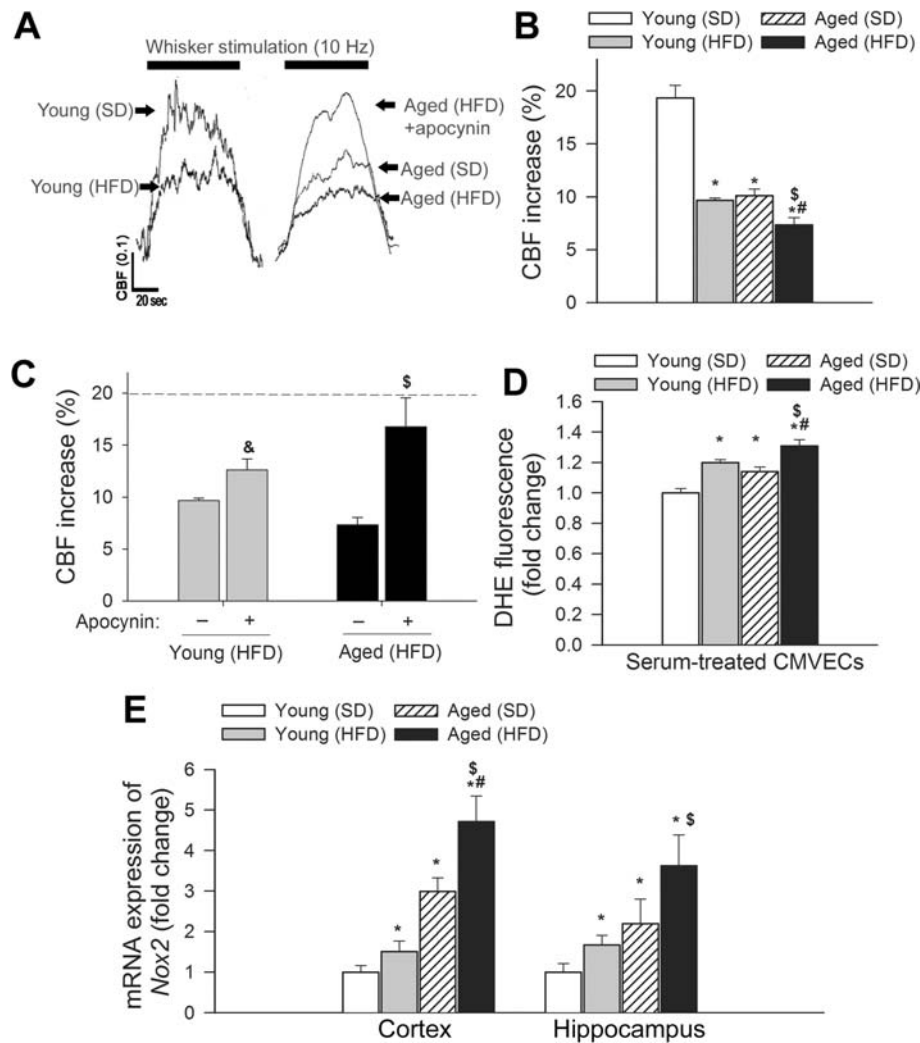


Figure 6. Obesity-induced neurovascular uncoupling and upregulation of NADPH oxidase in aged mice. (A) Representative traces of cerebral blood flow (CBF) measured with a laser Doppler probe above the whisker barrel cortex during contralateral whisker stimulation (1 min, 10 Hz) in young and aged mice fed an HFD or SD (0.1 AU corresponds to ~5% increase in CBF from baseline). Panel B depicts the summary data of the effect of HFD-induced obesity on CBF responses to whisker stimulation in young and aged mice. Data are given as mean \pm SEM ($n = 8$ in each group). * $p < .05$ vs young mice (SD), $^{\#}p < .05$ vs aged mice (SD), $^{\S}p < .05$ vs young mice (HFD). (C) Summary data of the effect of apocynin on CBF responses to whisker stimulation in HFD-fed young and aged mice. $p < .05$ vs young mice (HFD), $^{\S}p < .05$ vs aged mice (HFD). (D) Summary data showing flow cytometric analysis of dihydroethidium fluorescence (indicating reactive oxygen species production) in primary CMVECs treated with sera collected from young and aged mice fed an SD or an HFD. Data are given as means \pm SEM ($n = 6$ in each group). * $p < .05$ vs young mice (SD), $^{\#}p < .05$ vs aged mice (SD), $^{\S}p < .05$ vs young mice (HFD). (E) Effects of obesity on mRNA expression of NADPH oxidase subunit *Nox2* in the hippocampi and cerebral cortex of young and aged mice fed an SD or an HFD. Data are given as mean \pm SEM ($n = 5$ in each group). * $p < .05$ vs young mice (SD), $^{\#}p < .05$ vs aged mice (SD), $^{\S}p < .05$ vs young mice (HFD).

with increased oxidative or nitrosative stress in the aged brain (6,7). Obesity significantly increased 3-nitrotyrosine content in the cortex of aged mice (Supplementary Figure IV). These findings support the concept that aging exacerbates obesity-induced oxidative stress and that increased production of ROS by NADPH oxidases play an important role in obesity-induced cerebrovascular dysfunction in aging.

To substantiate the pro-oxidative microvascular effects of obesity-induced circulating factors, we assessed the effects of sera obtained from obese aged mice on cellular ROS production in cultured CMVECs using the dihydroethidium fluorescence method. To our knowledge, this is the first study to demonstrate that factors present in the circulation of obese aged

mice elicit significantly greater endothelial oxidative stress than factors present in the circulation of lean aged mice (Figure 6D).

We found that obesity in aging resulted in significantly increased mRNA expression of the NADPH oxidase subunit *Nox2* in the mouse cortex and hippocampus (Figure 6E), compared with young mice, extending previous findings (6,7). Aging in lean mice also increased *Nox2* expression, extending recent findings (31,54).

DISCUSSION

The results of this study suggest that aging exacerbates the deleterious cerebrovascular effects of obesity by

promoting cerebrovascular rarefaction and neurovascular uncoupling. We also show that cerebrovascular impairment in obese aged mice is associated with significant cognitive decline.

Our studies provide new evidence in support of the concept (7) that obesity in aging exacerbates hippocampal cognitive impairment in mice (Figure 1). These findings are consistent with the conclusions of clinical studies, which suggest that obesity is an important risk factor for cognitive impairment in the elderly population (2). In obesity, the adipose tissue exhibits enhanced inflammatory status, characterized by a marked proinflammatory shift in the secretome (28,55–58), which results in increased circulating levels of adipose-derived proinflammatory cytokines and chemokines in both experimental animals and humans (8,59). Previous studies provided evidence that aging exacerbates obesity-induced inflammation in the adipose tissue (28,60), which leads to an increased presence of proinflammatory adipokines in the bloodstream of aged obese mice (8). Circulating inflammatory mediators, derived from adipose tissue, readily reach the cerebral microcirculation and likely alter the function and phenotype of CMVECs.

Here, we demonstrate that cognitive impairment in obese aged mice is associated with significant decline in microvascular density both in the hippocampus and in the cortex (Figure 2). The hippocampus is a key brain region involved in learning and memory, one of the main regions affected in Alzheimer's disease, and it is known to be particularly vulnerable to ischemia. Importantly, the extent of hippocampal microvascular rarefaction and the extent of impairment of hippocampal-dependent cognitive function positively correlate (Figure 2G). Previous studies also demonstrate that rarefaction of the hippocampal microvasculature in various pathophysiological conditions predicts cognitive dysfunction in the absence of or preceding neurodegeneration (8,61). It is generally considered that cerebrovascular rarefaction contributes to a decline in CBF that reduces metabolic support for neural signaling, thereby promoting cognitive impairment (23,61–63). Indeed, in obese patients, cortical CBF is decreased, which correlates with memory impairment (64). Thus, future studies need to elucidate whether decreased capillary density in aged obese mice is associated with ischemic foci, which have a deleterious effect on cognitive function. In that regard, it is significant that obesity in aging appears to be associated with upregulation of certain hypoxia-inducible genes, including endoglin (65), in the hippocampi (Ungvari and Csiszar, unpublished data, 2013).

The mechanisms of obesity-induced microvascular rarefaction in aged mice are likely multifaceted. Pericytes have key roles in preservation of the structural integrity of the cerebral microcirculation (36), thus it is possible that the increased obesity-induced loss of pericyte coverage reported in our studies (Figure 3) contribute to microvascular rarefaction in brain of aged obese mice. The mechanisms

of increased pericyte loss in aged obese mice are presently unknown. Pericytes are sensitive to inflammation and to oxidative damage. Therefore, it is possible that exacerbated obesity-induced neuroinflammation and oxidative stress (8) contributes to increased pericyte loss in aged HFD-fed mice. Pericytes are also important cellular constituents of the blood–brain barrier, and recent studies demonstrate that pericyte deficiency in *Pdgfr β ^{+/-}* mice leads to significant impairment of blood–brain barrier function (53) and development of a vascular cognitive impairment-like syndrome. Thus, loss of pericytes (Figure 3) is likely to contribute to both microvascular rarefaction and blood–brain barrier disruption (8) in aged obese mice.

Impaired angiogenesis is another mechanism, likely involved in cerebrovascular rarefaction (66). Here, we demonstrate that in the mouse hippocampus, HFD appears to increase the angiogenesis gene expression signature (eg, increasing the expression of *Vegfa*, Supplementary Table II), and although age and the age–diet interaction appear to have mixed effects, the age–diet interaction shows a trend toward decreased angiogenic signature (Figure 4). On the basis of these data, we propose that a decline in proangiogenic stimuli is not the primary cause for age-related microvascular rarefaction in the cerebral circulation. Our findings also do not support the hypothesis that changes in serum levels of pro- and/or antiangiogenic factors contribute to microvascular rarefaction in aged obese mice. Accordingly, we found that treatment with sera obtained from aged obese mice actually increases, rather than decreases, endothelial angiogenic capacity (Figure 5). Recently, we demonstrated that obesity and aging are associated with an increased circulating level of adipose tissue-derived proinflammatory cytokines in mice (28). Many of these cytokines and growth factors exert proangiogenic effects, thus we attribute results of the serum treatment studies to the effects of these inflammatory mediators. In contrast, our recent studies confirm that primary CMVECs derived from aged rodents exhibit impaired angiogenic response to exogenous administration of vascular endothelial growth factor, suggesting that aged endothelial cells become resistant to vascular endothelial growth factor and other inducers of angiogenesis (41). It is possible that intrinsic angiogenic incompetence of endothelial cells contributes to microvascular rarefaction in aged obese mice. This hypothesis needs to be tested in future studies. The mechanisms responsible for age-related impairment of endothelial angiogenic capacity likely include dysregulation of *Dicer1* (ribonuclease III, a key enzyme of the miRNA machinery) (41) and *Nrf2*, a newly discovered regulator of endothelial angiogenic processes (43). This later concept is consistent with the findings that aging is associated with *Nrf2* dysfunction in endothelial cells (67,68) and that obesity exacerbates *Nrf2* dysfunction (7). Moreover, treatment with resveratrol, a potent activator of endothelial *Nrf2* activity, prevents HFD-induced endothelial apoptosis (46) and increases capillary density in the brain (69).

There are also increasing number of studies extant ascribing microvascular rarefaction to endothelial injury and apoptosis. Our previous studies provide evidence that feeding an HFD promotes endothelial apoptosis in aged mice (70) and that aged endothelial cells exhibit increased susceptibility to apoptosis induced by metabolic stressors (68). Nevertheless, further studies are needed to provide direct evidence for the role of increased microvascular apoptosis in microvascular rarefaction in obese aged mice.

In addition to microvascular rarefaction, the decrement of microvascular vasodilator function is also likely to contribute to impaired CBF and cognitive decline. This is the first study to demonstrate obesity-induced exacerbation of neurovascular uncoupling in a mouse model of aging that recapitulates cerebrovascular alterations and deficits of higher cortical function present in obese elderly humans. We demonstrate that aging leads to profound neurovascular dysregulation (54), characterized by impaired CBF responses induced by synaptic activity (Figure 6). Age-related impairment of neurovascular coupling is manifested in elderly patients (71–73) and has been causally linked to the decline in higher cortical functions including cognition (74,75). Here, we demonstrate for the first time that aging exacerbates obesity-induced decrease in neurovascular coupling. Significant impairment of a key homeostatic mechanism matching energy supply with the needs of active neuronal tissue likely has a profound negative effect on brain function in aging. Thus, it is logical to hypothesize that the neurovascular uncoupling contributes to the documented deleterious effects of obesity on cognitive function that is manifest in aged rodents (8) (Figure 1) and elderly humans. There is growing experimental evidence that endothelial NO production, in addition to neuronal NO, has an important role in neurovascular coupling (76–78). This concept is supported by our observation that inhibition of NO synthesis dramatically reduces neurovascular coupling in young mice (31). The findings, that in aged obese mice inhibition of endothelial NO synthesis did not decrease the CBF responses elicited by neuronal activity (data not shown), whereas inhibitions of NADPH oxidases restores neurovascular coupling (Figure 6), suggest that cerebrovascular endothelial dysfunction contributes to dysregulation of neurovascular coupling (31,54). Impairment of cerebrovascular endothelial function by obesity can also be anticipated based on its documented deleterious effect on endothelial function in large vessels of aged mice (28,70). It should be noted that obesity per se impairs NO mediation of neurovascular coupling suggesting that negative cerebral effects of cardiovascular risk factors should not be ignored even in the young mice. The mechanism by which aging and obesity impair endothelial function involves an increased breakdown of NO by elevated levels of ROS. Multiple lines of evidence support this concept. First, aging is associated with increased ROS production in microvessels both in the brain and in other vascular beds (54,79). Previous studies suggest that increased activity/expression of NADPH

oxidases contribute to aging-induced microvascular oxidative stress (54). Second, aging upregulates NADPH oxidase expression in the brain (31), and this effect is exacerbated in the presence of obesity (Figure 6E). Third, in the microcirculation of aged rodents, endothelium-derived NO was shown to react with NADPH oxidase-derived O_2^- forming $ONOO^-$, thus decreasing the bioavailability of NO (79,80). Aged mouse brains exhibit an increased 3-nitrotyrosine content (31), a biomarker of increased $ONOO^-$ formation, suggesting that impaired endothelial mediation of cerebrovascular dilation in aging is due to increased scavenging of vasodilator NO (54). Importantly, 3-nitrotyrosine content is significantly increased in the brains of obese aged animals (31). Our findings are also consistent with the conclusions of recent studies suggesting that NOX2-derived superoxide plays a major role in endothelial dysfunction produced by an HFD (81).

Collectively, our present and previous studies demonstrate that obesity exerts deleterious cerebrovascular effects in aged mice, promoting cerebrovascular rarefaction and neurovascular uncoupling. The morphological and functional impairment of the cerebral microvasculature, in association with increased blood–brain barrier disruption and neuroinflammation (8), likely contribute to obesity-induced cognitive decline in aging.

SUPPLEMENTARY MATERIAL

Supplementary material can be found at: <http://biomedgerontology.oxfordjournals.org/>

FUNDING

This work was supported by grants from the American Heart Association (to Z.T., P.T., A.C., and Z.U.), the National Center for Complementary and Alternative Medicine (R01-AT006526 to Z.U.), the National Institute on Aging (AG031085 to A.C.; AG038747 to W.E.S.), the American Federation for Aging Research (to A.C.), the Oklahoma Center for the Advancement of Science and Technology (to A.C., Z.U., W.E.S.), Hungarian Scientific Research Fund (OTKA-K108444), the Nemzeti Fejlesztési Ügynökség (Developing Competitiveness of Universities in the South Transdanubian Region, “Identification of new biomarkers,” SROP-4.2.2.A-11/1/KONV-2012-0017 and “Complex examination of neuropeptides” SROP-4.2.2.A-11/1/KONV-2012-0024 to A.K.), and the Ellison Medical Foundation (to W.E.S.).

CONFLICT OF INTEREST

None.

REFERENCES

1. Wang YC, Colditz GA, Kuntz KM. Forecasting the obesity epidemic in the aging U.S. population. *Obesity (Silver Spring)*. 2007;15:2855–2865.
2. Wolf PA, Beiser A, Elias MF, Au R, Vasani RS, Seshadri S. Relation of obesity to cognitive function: importance of central obesity and synergistic influence of concomitant hypertension. The Framingham Heart Study. *Curr Alzheimer Res*. 2007;4:111–116.
3. Gustafson DR, Karlsson C, Skoog I, Rosengren L, Lissner L, Blennow K. Mid-life adiposity factors relate to blood-brain barrier integrity in late life. *J Intern Med*. 2007;262:643–650.
4. Beydoun MA, Beydoun HA, Wang Y. Obesity and central obesity as risk factors for incident dementia and its subtypes: a systematic review and meta-analysis. *Obes Rev*. 2008;9:204–218.

5. Alosco ML, Spitznagel MB, Raz N, et al. Obesity interacts with cerebral hypoperfusion to exacerbate cognitive impairment in older adults with heart failure. *Cerebrovasc Dis Extra*. 2012;2:88–98.
6. Bruce-Keller AJ, White CL, Gupta S, et al. NOX activity in brain aging: exacerbation by high fat diet. *Free Radic Biol Med*. 2010;49:22–30.
7. Morrison CD, Pistell PJ, Ingram DK, et al. High fat diet increases hippocampal oxidative stress and cognitive impairment in aged mice: implications for decreased Nrf2 signaling. *J Neurochem*. 2010;114:1581–1589.
8. Tucsek Z, Toth P, Sosnowska D, et al. Obesity in aging exacerbates blood brain barrier disruption, neuroinflammation and oxidative stress in the mouse hippocampus: effects on expression of genes involved in beta-amyloid generation and Alzheimer's disease. *J Gerontol Biol Med Sci*. 2013. doi:10.1093/gerona/glt177
9. Beavers KM, Hsu FC, Houston DK, et al.; Health ABC Study. The role of metabolic syndrome, adiposity, and inflammation in physical performance in the Health ABC Study. *J Gerontol A Biol Sci Med Sci*. 2013;68:617–623.
10. Scuteri A, Najjar SS, Muller DC, et al. Metabolic syndrome amplifies the age-associated increases in vascular thickness and stiffness. *J Am Coll Cardiol*. 2004;43:1388–1395.
11. Brinkley TE, Hsu FC, Beavers KM, et al. Total and abdominal adiposity are associated with inflammation in older adults using a factor analysis approach. *J Gerontol A Biol Sci Med Sci*. 2012;67:1099–1106.
12. Sloboda N, Fève B, Thornton SN, et al. Fatty acids impair endothelium-dependent vasorelaxation: a link between obesity and arterial stiffness in very old Zucker rats. *J Gerontol A Biol Sci Med Sci*. 2012;67:927–938.
13. Gorelick PB, Scuteri A, Black SE, et al.; American Heart Association Stroke Council, Council on Epidemiology and Prevention, Council on Cardiovascular Nursing, Council on Cardiovascular Radiology and Intervention, and Council on Cardiovascular Surgery and Anesthesia. Vascular contributions to cognitive impairment and dementia: a statement for healthcare professionals from the American heart association/American stroke association. *Stroke*. 2011;42:2672–2713.
14. Gustafson DR. Adiposity and cognitive decline: underlying mechanisms. *J Alzheimers Dis*. 2012;30(suppl 2):S97–112.
15. Kivipelto M, Ngandu T, Fratiglioni L, et al. Obesity and vascular risk factors at midlife and the risk of dementia and Alzheimer disease. *Arch Neurol*. 2005;62:1556–1560.
16. Maesako M, Uemura K, Kubota M, et al. Exercise is more effective than diet control in preventing high fat diet-induced β -amyloid deposition and memory deficit in amyloid precursor protein transgenic mice. *J Biol Chem*. 2012;287:23024–23033.
17. Zlokovic BV. Neurovascular pathways to neurodegeneration in Alzheimer's disease and other disorders. *Nat Rev Neurosci*. 2011;12:723–738.
18. Lin AL, Zheng W, Halloran JJ, et al. Chronic rapamycin restores brain vascular integrity and function through NO synthase activation and improves memory in symptomatic mice modeling Alzheimer's disease. *J Cereb Blood Flow Metab*. 2013;33:1412–1421.
19. García-Amado M, Prensa L. Stereological analysis of neuron, glial and endothelial cell numbers in the human amygdaloid complex. *PLoS One*. 2012;7:e38692.
20. Ingraham JP, Forbes ME, Riddle DR, Sonntag WE. Aging reduces hypoxia-induced microvascular growth in the rodent hippocampus. *J Gerontol A Biol Sci Med Sci*. 2008;63:12–20.
21. Khan AS, Lynch CD, Sane DC, Willingham MC, Sonntag WE. Growth hormone increases regional coronary blood flow and capillary density in aged rats. *J Gerontol A Biol Sci Med Sci*. 2001;56:B364–B371.
22. Sonntag WE, Lynch C, Thornton P, Khan A, Bennett S, Ingram R. The effects of growth hormone and IGF-1 deficiency on cerebrovascular and brain ageing. *J Anat*. 2000;197 Pt 4:575–585.
23. Sonntag WE, Lynch CD, Cooney PT, Hutchins PM. Decreases in cerebral microvasculature with age are associated with the decline in growth hormone and insulin-like growth factor 1. *Endocrinology*. 1997;138:3515–3520.
24. Warrington JP, Csiszar A, Johnson DA, et al. Cerebral microvascular rarefaction induced by whole brain radiation is reversible by systemic hypoxia in mice. *Am J Physiol Heart Circ Physiol*. 2011;300:H736–H744.
25. Warrington JP, Csiszar A, Mitschelen M, Lee YW, Sonntag WE. Whole brain radiation-induced impairments in learning and memory are time-sensitive and reversible by systemic hypoxia. *PLoS One*. 2012;7:e30444.
26. Attwell D, Buchan AM, Charpak S, Lauritzen M, Macvicar BA, Newman EA. Glial and neuronal control of brain blood flow. *Nature*. 2010;468:232–243.
27. Li W, Prakash R, Chawla D, et al. Early effects of high-fat diet on neurovascular function and focal ischemic brain injury. *Am J Physiol Regul Integr Comp Physiol*. 2013;304:R1001–R1008.
28. Bailey-Downs LC, Tucsek Z, Toth P, et al. Aging exacerbates obesity-induced oxidative stress and inflammation in perivascular adipose tissue in mice: a paracrine mechanism contributing to vascular redox dysregulation and inflammation. *J Gerontol A Biol Sci Med Sci*. 2013;68:780–792.
29. Carrié I, Debray M, Bourre JM, Francès H. Age-induced cognitive alterations in OF1 mice. *Physiol Behav*. 1999;66:651–656.
30. Toth P, Tucsek Z, Sosnowska D, et al. Age-related autoregulatory dysfunction and cerebrovascular injury in mice with angiotensin II-induced hypertension. *J Cereb Blood Flow Metab*. 2013;33:1732–1742.
31. Toth P, Tarantini S, Tucsek Z, et al. Resveratrol treatment rescues neurovascular coupling in aged mice: role of improved cerebrovascular endothelial function and downregulation of NADPH oxidase. *Am J Physiol Heart Circ Physiol*. 2014;306:H299–H308.
32. Csiszar A, Smith K, Labinskyy N, Orosz Z, Rivera A, Ungvari Z. Resveratrol attenuates TNF-alpha-induced activation of coronary arterial endothelial cells: role of NF-kappaB inhibition. *Am J Physiol Heart Circ Physiol*. 2006;291:H1694–H1699.
33. Zhang H, Zhang J, Ungvari Z, Zhang C. Resveratrol improves endothelial function: role of TNF[alpha] and vascular oxidative stress. *Arterioscler Thromb Vasc Biol*. 2009;29:1164–1171.
34. Kazama K, Anrather J, Zhou P, et al. Angiotensin II impairs neurovascular coupling in neocortex through NADPH oxidase-derived radicals. *Circ Res*. 2004;95:1019–1026.
35. Hof PR, Young WC, Bloom FE, Belichenko PV, Celio MR. *Comparative Cytoarchitectonic Atlas of the C57BL/6 and 129/Sv Mouse Brains*. New York, NY: Elsevier; 2000.
36. Winkler EA, Bell RD, Zlokovic BV. Central nervous system pericytes in health and disease. *Nat Neurosci*. 2011;14:1398–1405.
37. Csiszar A, Tucsek Z, Toth P, et al. Synergistic effects of hypertension and aging on cognitive function and hippocampal expression of genes involved in β -amyloid generation and Alzheimer's disease. *Am J Physiol Heart Circ Physiol*. 2013;305:H1120–H1130.
38. Bailey-Downs LC, Mitschelen M, Sosnowska D, et al. Liver-specific knockdown of IGF-1 decreases vascular oxidative stress resistance by impairing the Nrf2-dependent antioxidant response: a novel model of vascular aging. *J Gerontol A Biol Sci Med Sci*. 2012;67:313–329.
39. Dvinge H, Bertone P. HTqPCR: high-throughput analysis and visualization of quantitative real-time PCR data in R. *Bioinformatics*. 2009;25:3325–3326.
40. Subramanian A, Tamayo P, Mootha VK, et al. Gene set enrichment analysis: a knowledge-based approach for interpreting genome-wide expression profiles. *Proc Natl Acad Sci USA*. 2005;102:15545–15550.
41. Ungvari Z, Tucsek Z, Sosnowska D, et al. Aging-induced dysregulation of dicer1-dependent microRNA expression impairs angiogenic capacity of rat cerebrovascular endothelial cells. *J Gerontol A Biol Sci Med Sci*. 2013;68:877–891.
42. Csiszar A, Sosnowska D, Tucsek Z, et al. Circulating factors induced by caloric restriction in the nonhuman primate *Macaca mulatta* activate angiogenic processes in endothelial cells. *J Gerontol A Biol Sci Med Sci*. 2013;68:235–249.

43. Valcarcel-Ares MN, Gautam T, Warrington JP, et al. Disruption of Nrf2 signaling impairs angiogenic capacity of endothelial cells: implications for microvascular aging. *J Gerontol A Biol Sci Med Sci*. 2012;67:821–829.
44. Tucsek Z, Gautam T, Sonntag WE, et al. Aging exacerbates microvascular endothelial damage induced by circulating factors present in the serum of septic patients. *J Gerontol A Biol Sci Med Sci*. 2013;68:652–660.
45. Ungvari Z, Labinskyy N, Mukhopadhyay P, et al. Resveratrol attenuates mitochondrial oxidative stress in coronary arterial endothelial cells. *Am J Physiol Heart Circ Physiol*. 2009;297:H1876–H1881.
46. Ungvari Z, Bagi Z, Feher A, et al. Resveratrol confers endothelial protection via activation of the antioxidant transcription factor Nrf2. *Am J Physiol Heart Circ Physiol*. 2010;299:H18–H24.
47. Ungvari Z, Bailey-Downs L, Gautam T, et al. Adaptive induction of NF-E2-related factor-2-driven antioxidant genes in endothelial cells in response to hyperglycemia. *Am J Physiol Heart Circ Physiol*. 2011;300:H1133–H1140.
48. Csiszar A, Labinskyy N, Perez V, et al. Endothelial function and vascular oxidative stress in long-lived GH/IGF-deficient Ames dwarf mice. *Am J Physiol Heart Circ Physiol*. 2008;295:H1882–H1894.
49. Bailey-Downs LC, Sosnowska D, Toth P, et al. Growth hormone and IGF-1 deficiency exacerbate high-fat diet-induced endothelial impairment in obese Lewis dwarf rats: implications for vascular aging. *J Gerontol A Biol Sci Med Sci*. 2012;67:553–564.
50. Csiszar A, Podlutzky A, Podlutzkaya N, et al. Testing the oxidative stress hypothesis of aging in primate fibroblasts: is there a correlation between species longevity and cellular ROS production? *J Gerontol A Biol Sci Med Sci*. 2012;67:841–852.
51. Ungvari Z, Sosnowska D, Podlutzky A, Koncz P, Sonntag WE, Csiszar A. Free radical production, antioxidant capacity, and oxidative stress response signatures in fibroblasts from Lewis Dwarf rats: effects of life span-extending peripubertal GH treatment. *J Gerontol A Biol Sci Med Sci*. 2011;66:501–510. doi:10.1093/gerona/glr004
52. Stenholm S, Sallinen J, Koster A, et al. Association between obesity history and hand grip strength in older adults—exploring the roles of inflammation and insulin resistance as mediating factors. *J Gerontol A Biol Sci Med Sci*. 2011;66:341–348.
53. Bell RD, Winkler EA, Sagare AP, et al. Pericytes control key neurovascular functions and neuronal phenotype in the adult brain and during brain aging. *Neuron*. 2010;68:409–427.
54. Park L, Anrather J, Girouard H, Zhou P, Iadecola C. Nox2-derived reactive oxygen species mediate neurovascular dysregulation in the aging mouse brain. *J Cereb Blood Flow Metab*. 2007;27:1908–1918.
55. Surmi BK, Hasty AH. Macrophage infiltration into adipose tissue: initiation, propagation and remodeling. *Future Lipidol*. 2008;3:545–556.
56. Fain JN. Release of interleukins and other inflammatory cytokines by human adipose tissue is enhanced in obesity and primarily due to the nonfat cells. *Vitam Horm*. 2006;74:443–477.
57. Hocking SL, Wu LE, Guilhaus M, Chisholm DJ, James DE. Intrinsic depot-specific differences in the secretome of adipose tissue, preadipocytes, and adipose tissue-derived microvascular endothelial cells. *Diabetes*. 2010;59:3008–3016.
58. Nishimura S, Manabe I, Nagasaki M, et al. In vivo imaging in mice reveals local cell dynamics and inflammation in obese adipose tissue. *J Clin Invest*. 2008;118:710–721.
59. Cartier A, Côté M, Lemieux I, et al. Age-related differences in inflammatory markers in men: contribution of visceral adiposity. *Metabolism*. 2009;58:1452–1458.
60. Wu D, Ren Z, Pae M, et al. Aging up-regulates expression of inflammatory mediators in mouse adipose tissue. *J Immunol*. 2007;179:4829–4839.
61. Troen AM, Shea-Budgell M, Shukitt-Hale B, Smith DE, Selhub J, Rosenberg IH. B-vitamin deficiency causes hyperhomocysteinemia and vascular cognitive impairment in mice. *Proc Natl Acad Sci U S A*. 2008;105:12474–12479.
62. Khan AS, Sane DC, Wannenburg T, Sonntag WE. Growth hormone, insulin-like growth factor-1 and the aging cardiovascular system. *Cardiovasc Res*. 2002;54:25–35.
63. Riddle DR, Sonntag WE, Lichtenwalner RJ. Microvascular plasticity in aging. *Ageing Res Rev*. 2003;2:149–168.
64. Birdsill AC, Carlsson CM, Willette AA, et al. Low cerebral blood flow is associated with lower memory function in metabolic syndrome. *Obesity (Silver Spring)*. 2013;21:1313–1320.
65. Zhu Y, Sun Y, Xie L, Jin K, Sheibani N, Greenberg DA. Hypoxic induction of endoglin via mitogen-activated protein kinases in mouse brain microvascular endothelial cells. *Stroke*. 2003;34:2483–2488.
66. Ungvari Z, Kaley G, de Cabo R, Sonntag WE, Csiszar A. Mechanisms of vascular aging: new perspectives. *J Gerontol A Biol Sci Med Sci*. 2010;65:1028–1041.
67. Ungvari Z, Bailey-Downs L, Gautam T, et al. Age-associated vascular oxidative stress, Nrf2 dysfunction, and NF- κ B activation in the nonhuman primate *Macaca mulatta*. *J Gerontol A Biol Sci Med Sci*. 2011;66:866–875.
68. Ungvari Z, Bailey-Downs L, Sosnowska D, et al. Vascular oxidative stress in aging: a homeostatic failure due to dysregulation of NRF2-mediated antioxidant response. *Am J Physiol Heart Circ Physiol*. 2011;301:H363–H372.
69. Oomen CA, Farkas E, Roman V, van der Beek EM, Luiten PG, Meerlo P. Resveratrol preserves cerebrovascular density and cognitive function in aging mice. *Front Aging Neurosci*. 2009;1:4.
70. Pearson KJ, Baur JA, Lewis KN, et al. Resveratrol delays age-related deterioration and mimics transcriptional aspects of dietary restriction without extending life span. *Cell Metab*. 2008;8:157–168.
71. Zaletel M, Struel M, Pretnar-Oblak J, Zvan B. Age-related changes in the relationship between visual evoked potentials and visually evoked cerebral blood flow velocity response. *Funct Neurol*. 2005;20:115–120.
72. Topcuoglu MA, Aydin H, Saka E. Occipital cortex activation studied with simultaneous recordings of functional transcranial Doppler ultrasound (fTCD) and visual evoked potential (VEP) in cognitively normal human subjects: effect of healthy aging. *Neurosci Lett*. 2009;452:17–22.
73. Stefanova I, Stephan T, Becker-Bense S, Dera T, Brandt T, Dieterich M. Age-related changes of blood-oxygen-level-dependent signal dynamics during optokinetic stimulation. *Neurobiol Aging*. 2013;34:2277–2286.
74. Sorond FA, Hurwitz S, Salat DH, Greve DN, Fisher ND. Neurovascular coupling, cerebral white matter integrity, and response to cocoa in older people. *Neurology*. 2013;81:904–909.
75. Sorond FA, Kiely DK, Galica A, et al. Neurovascular coupling is impaired in slow walkers: the MOBILIZE Boston Study. *Ann Neurol*. 2011;70:213–220.
76. Girouard H, Park L, Anrather J, Zhou P, Iadecola C. Cerebrovascular nitrosative stress mediates neurovascular and endothelial dysfunction induced by angiotensin II. *Arterioscler Thromb Vasc Biol*. 2007;27:303–309.
77. Stobart JL, Lu L, Anderson HD, Mori H, Anderson CM. Astrocyte-induced cortical vasodilation is mediated by D-serine and endothelial nitric oxide synthase. *Proc Natl Acad Sci U S A*. 2013;110:3149–3154.
78. Longden T, Nelson M. Recruitment of the vascular endothelium into neurovascular coupling. *Proceedings of the British Pharmacological Society. The FASEB Journal*. 2012;26:842.4.
79. Csiszar A, Ungvari Z, Edwards JG, et al. Aging-induced phenotypic changes and oxidative stress impair coronary arteriolar function. *Circ Res*. 2002;90:1159–1166.
80. Pacher P, Beckman JS, Liaudet L. Nitric oxide and peroxynitrite in health and disease. *Physiol Rev*. 2007;87:315–424.
81. Lynch CM, Kinzenbaw DA, Chen X, et al. Nox2-derived superoxide contributes to cerebral vascular dysfunction in diet-induced obesity. *Stroke*. 2013;44:3195–3201.